The AAPS Journal (2023) 25:1
https://doi.org/10.1208/s12248-022-00765-3

RESEARCH ARTICLE

A Simple One-Parameter Percent Dissolved *Versus* Time Dissolution Equation that Accommodates Sink and Non-sink Conditions *via* Drug Solubility and Dissolution Volume

James E. Polli[1]

Received: 19 August 2022 / Accepted: 26 October 2022 / Published online: 17 November 2022

Abstract
In vitro dissolution generally involves sink conditions, so dissolution equations generally do not need to accommodate non-sink conditions. Greater use of biorelevant media, which are typically less able to provide sink conditions than pharmaceutical surfactants, necessitates equations that accommodate non-sink conditions. One objective was to derive an integrated, one-parameter dissolution equation for percent dissolved *versus* time that accommodates non-sink effects *via* drug solubility and dissolution volume parameters, including incomplete solubility. A second objective was to characterize the novel equation by fitting it to biorelevant dissolution profiles of tablets of two poorly water-soluble drugs, as well as by conducting simulations of the effect of dose on dissolution profile. The Polli dissolution equation was derived, $\% \; dissolved = 100\% \left[1 - \frac{(M_0 - c_s V)}{M_0 - c_s V e^{-k_d \left(\frac{M_0 - c_s V}{V} \right) t}} \right]$, where M_0 is the drug dose (mg), c_s is drug solubility (mg/ml), V is dissolution volume (ml), and k_d is dissolution rate coefficient (ml/mg per min). Maximum allowable percent dissolved was determined by drug solubility and not a fitted extent of dissolution parameter. The equation fit tablet profiles in the presence and absence of sink conditions, using a single fitted parameter, k_d, and where solubility ranged over a 1000-fold range. k_d was generally smaller when c_s was larger. FeSSGF provided relatively small k_d values, reflecting FeSSGF colloids are large and slowly diffusing. Simulations showed impact of non-sink conditions, as well as plausible k_d values for various c_s scenarios, in agreement with observed k_d values. The equation has advantages over first-order and *z*-factor dissolution rate equations. An Excel file for regression is provided.

Keywords Dissolution · Solubility · Sink condition · Model · Dose

Introduction

Immediate-release (IR) *in vitro* dissolution media generally provide sink conditions, or at least 85% dissolution in 60 min (1). For example, United States Pharmacopeia (USP) dissolution of capsules of the poorly water-soluble drug aprepitant employs 2.2% sodium lauryl sulfate (SLS) and a time specification at either 20 or 30 min, depending on the test (i.e., test 1, 2, or 3) (2). Aprepitant solubility without surfactant is only 3–7 µg/ml between pH 2–10 (3).

Because of this general practice of dissolution being designed to allow 85% or more dissolution, dissolution equations that are applied to percent dissolved *versus* time profiles often do not accommodate sink conditions (4–11). These equations are generally designed for 100% dissolution, like the *in vitro* test. Of course, these dissolution equations, particularly those in the simple analytical form percent dissolved as a function of time, have also been modified to allow for fitting of an extent of dissolution parameter when dissolution is incomplete (5, 6, 12, 13). Dissolution equations that are only available in differential equation (i.e., not in analytical or integrated form, such as *z*-factor dissolution rate equation for potential non-sink conditions) are not simple in that they cannot employ regression to fit to dissolution data, but rather require numerical integration (e.g., Runge–Kutta method using STELLA software) (14–17).

With the greater utilization of biorelevant media, there is a need for simple *in vitro* dissolution equations that accommodate and consider non-sink conditions, including incomplete dissolution due to insufficient solubility of all

✉ James E. Polli
jpolli@rx.umaryland.edu

[1] University of Maryland School of Pharmacy, 20 Penn Street, N623, Baltimore, Maryland 21201, USA

drug dose. Biorelevant media, with a composition that is intended to mimic luminal chyme properties, often provides a lower drug solubility than do pharmaceutical surfactants or a pH selection in routine *in vitro* dissolution. For example, the solubility of each of the weakly acidic, poorly soluble drugs indomethacin, sulindac, ibuprofen, and naproxen was enhanced less than twofold in Fasted State Simulated Intestinal Fluid-Version 2 (FaSSIF-V2, pH 6.5), compared to buffer (18). Meanwhile, the USP medium for indomethacin capsules, sulindac tablets, ibuprofen tablets, and naproxen tablets is pH 7.2 or 7.4 phosphate buffer (2). Similarly, celecoxib is a poorly water-soluble weak acid where only about 5–15% of a 200 mg celecoxib dose dissolves in pH 6.8 phosphate buffer (19) or FaSSIF-V2 (20). Meanwhile, tier 1 regulatory dissolution of celecoxib capsules employs pH 12 sodium phosphate with 1% SLS (21).

More frequent use of biorelevant media will require dissolution equations, preferably simple equations without the need for numerical integration, that can accommodate non-sink conditions. Consistent with this perspective is that, for poorly water-soluble drugs, drug permeation across the gastrointestinal tract occurs even when drug is incompletely dissolved, allowing for subsequent additional drug dissolution (22). I am unaware of a simple (i.e., non-differential) dissolution equation for percent dissolved *versus* time that accommodates non-sink conditions *via* drug solubility and dissolution volume. For example, no such equation is listed in Polli *et al*. or Costa and Lobo (5, 6).

One objective was to derive an integrated (i.e., not differential), one-parameter dissolution equation for percent dissolved *versus* time that considered non-sink effects. Here, a one-parameter dissolution equation means that only one parameter (denoted the dissolution rate coefficient, k_d) is fitted in regressing the equation to the dissolution data, without the need for a fitted extent of dissolution parameter. A second objective was to characterize the novel dissolution equation by fitting the equation to biorelevant dissolution profiles of tablets of two poorly water-soluble drugs with the same 200 mg strength, as well as by conducting simulations of the effect of dose. The two drugs were ibuprofen and ketoconazole, which are a weak acid and weak base, respectively. Biorelevant media were Fasted State Simulated Gastric Fluid (FaSSGF), FaSSIF-V2, Fed State Simulated Gastric Fluid (FeSSGF), and Fed State Simulated Intestinal Fluid-Version 2 (FeSSIF-V2), where drug solubility ranged over 1000-fold.

Results indicate that an equation for percent dissolved *versus* time was derived, where the maximum allowable percent dissolved was determined by drug dose, drug solubility, and dissolution volume. The equation was able to fit ibuprofen and ketoconazole tablet dissolution profiles. As perhaps expected, the dissolution rate coefficient k_d was generally smaller when drug solubility (c_s) was larger. However, FeSSGF provided relatively small k_d values, reflecting that FeSSGF colloids are large and slowly diffusing. Simulations of the effect of dose on dissolution profile revealed the expected impact of non-sink conditions, as well as plausible k_d values for various c_s scenarios, in agreement with observed k_d values. The derived equation, with only a one fitted parameter, will have practical utility in fitting percent dissolved *versus* time profiles, including when non-sink conditions prevail. The derived equation is simple, in that it is an integrated form and is not a differential equation, such that only non-linear regression and not numerical integration is needed to fit the equation to dissolution data. An Excel file for regression is provided.

Theoretical

Derivation of Polli Dissolution Equation

A novel equation is derived for drug dissolution. The equation (i.e., Eq. 21 below) is an applied equation, in that the equation is anticipated to be practically applied to percent dissolved *versus* time profiles.

Drug dissolution rate is assumed to proceed, in part, due to the amount of drug that is not dissolved, i.e.:

$$dM/dt \propto -M \tag{1}$$

where M is the mass undissolved. The familiar first-order dissolution equation also considers undissolved mass as the driving force of dissolution.

A potential barrier to the rate of dissolution is lack of sink conditions. M_0 is the drug dose (i.e., $M = M_0$ at $t = 0$), not all of which may potentially dissolved if drug solubility (c_s) and/or dissolution volume (V) is too low. That is, if c_s and/or V is excessively low, M_0 may not completely dissolve at even infinite time. Hence, an additional familiar impact on drug dissolution rate is the gradient between drug solubility and drug bulk concentration, i.e.:

$$dM/dt \propto -\left(c_s - \frac{M_0 - M}{V}\right) \tag{2}$$

Non-sink conditions are not explicitly defined here, although non-sink conditions is a familiar concept where bulk drug concentration becomes sufficiently high relative to c_s (e.g., over 33%), such that dissolution rate is hindered.

Considering these two factors (i.e., Eqs. 1 and 2), drug dissolution rate is:

$$dM/dt = -k_d M\left(c_s - \frac{M_0 - M}{V}\right) \tag{3}$$

Interestingly, while the above two factors are familiar factors in dissolution equation, I am unaware of Eq. 3 as an expression

for dissolution rate, or the availability of its solution (e.g., Eqs. 18 or 21 below). Equation 3 differs from the well known, and certainly more fundamental, film equation (i.e., Fick's first law):

$$dM/dt = -\frac{AD}{h}(c_s - c_b)$$

where A, D, h, and c_b are area, diffusivity, film thickness, and drug bulk concentration, respectively. While this difference between Eq. 3 and Fick's first law may appear modest, Fick's first law is certainly more fundamental, while Eq. 3, per below, has novel practical application in fitting dissolution profiles.

In order to solve Eq. 3:

$$dM/dt = -\frac{k_d}{V}M(c_sV - M_0 + M) \tag{4}$$

$$\frac{dM}{M(c_sV - M_0 + M)} = -\frac{k_d}{V}dt \tag{5}$$

$$\frac{1}{c_sV - M_0}\left(\frac{1}{M} - \frac{1}{c_sV - M_0 + M}\right)dM = -\frac{k_d}{V}dt \tag{6}$$

$$\left(\frac{1}{M} - \frac{1}{c_sV - M_0 + M}\right)dM = -k_d\left(\frac{c_sV - M_0}{V}\right)dt \tag{7}$$

Integrating yields:

$$\ln|M| - \ln|c_sV - M_0 + M| = -k_d\left(\frac{c_sV - M_0}{V}\right)t + C \tag{8}$$

$$\ln\left|\frac{M}{c_sV - M_0 + M}\right| = -k_d\left(\frac{c_sV - M_0}{V}\right)t + C \tag{9}$$

$$\frac{M}{c_sV - M_0 + M} = Ae^{-k_d\left(\frac{c_sV - M_0}{V}\right)t} \tag{10}$$

Substituting $M = M_0$ at $t = 0$ yields:

$$A = \frac{M_0}{c_sV}$$

$$\frac{M}{c_sV - M_0 + M} = \frac{M_0}{c_sV}e^{-k_d\left(\frac{c_sV - M_0}{V}\right)t} \tag{11}$$

$$\frac{c_sV - M_0 + M}{M} = \frac{c_sV}{M_0}e^{k_d\left(\frac{c_sV - M_0}{V}\right)t} \tag{12}$$

$$\frac{c_sV - M_0}{M} = \frac{c_sV}{M_0}e^{k_d\left(\frac{c_sV - M_0}{V}\right)t} - 1 \tag{13}$$

$$\frac{M}{c_sV - M_0} = \frac{1}{\frac{c_sV}{M_0}e^{k_d\left(\frac{c_sV - M_0}{V}\right)t} - 1} \tag{14}$$

$$M = \frac{c_sV - M_0}{\frac{c_sV}{M_0}e^{k_d\left(\frac{c_sV - M_0}{V}\right)t} - 1} \tag{15}$$

With a view to simplify where $M = M_0$ at $t = 0$:

$$M = \frac{(c_sV - M_0)M_0}{c_sVe^{k_d\left(\frac{c_sV - M_0}{V}\right)t} - M_0} \tag{16}$$

$$M = \frac{(M_0 - c_sV)M_0}{M_0 - c_sVe^{k_d\left(\frac{c_sV - M_0}{V}\right)t}} \tag{17}$$

$$M = \frac{(M_0 - c_sV)M_0}{M_0 - c_sVe^{-k_d\left(\frac{M_0 - c_sV}{V}\right)t}} \tag{18}$$

Hence, $M = M_0$ at $t = 0$, and $M = M_0 - c_sV$ at $t =$ infinite time.

As M is the mass undissolved, expressing dissolution in terms of mass dissolved (M_d) and percent dissolved (% dissolved):

$$M_d = M_0 - \frac{(M_0 - c_sV)M_0}{M_0 - c_sVe^{-k_d\left(\frac{M_0 - c_sV}{V}\right)t}} \tag{19}$$

$$M_d = M_0\left[1 - \frac{(M_0 - c_sV)}{M_0 - c_sVe^{-k_d\left(\frac{M_0 - c_sV}{V}\right)t}}\right] \tag{20}$$

$$\%dissolved = 100\%\left[1 - \frac{(M_0 - c_sV)}{M_0 - c_sVe^{-k_d\left(\frac{M_0 - c_sV}{V}\right)t}}\right] \tag{21}$$

Of note, Eqs. 11–21 are solutions to Eq. 3, the differential form of this Polli dissolution equation. Equation 21 is the solution form of Eq. 3 that directly reflects percent dissolved *versus* time and denoted the Polli dissolution equation. k_d is the only fitted parameter, with the expectation that M_0, c_s, and V are known.

The Polli Dissolution Equation Under Sink Condition: Collinearity of k_d and c_s

Under sink conditions (i.e., $c_s >> \frac{M_0 - M}{V}$), Eq. 3 yields:

$$dM/dt = -k_dMc_s \tag{22}$$

$$\frac{dM/dt}{M} = -k_d c_s \tag{23}$$

Similarly, under sink conditions (i.e., $M_0 << c_s V$), Eq. 21 yields:

$$\%\ dissolved = 100\%\left(1 - e^{-k_d c_s t}\right) \tag{24}$$

Hence, when sink conditions prevail (e.g., during at least initial dissolution), the value of k_d will be impacted by the value of c_s, as the two parameters are collinear.

Methods

Application to Ibuprofen 200 mg and Ketoconazole 200 mg Tablet Dissolution Profiles

Ibuprofen and ketoconazole IR tablets were selected as model drug products since they have the same dose (i.e., 200 mg) but differ in solubility profile, in part since ibuprofen is a weak acid and ketoconazole is a weak base. IR tablets were selected to maximize the impact of drug dose and drug solubility on dissolution profile (i.e., IR tablets were selected to minimize the impact of formulation on dissolution profile). That said, it is recognized that IR formulation (e.g., excipients, process) can impact dissolution, and that ibuprofen 200 mg (Major Pharmaceuticals, Livonia, MI) and ketoconazole 200 mg tablets (Teva Generics, Pomona, NY) differ in formulation, such their differing dissolution profiles may reflect differing formulation, in addition to differing drug solubilities. Ibuprofen tablets include excipients colloidal silicon dioxide, corn starch, croscarmellose sodium, hypromellose, iron oxide red, iron oxide yellow, microcrystalline cellulose, polyethylene glycol, polysorbate 80, stearic acid, and titanium oxide (23). Ketoconazole tablets include excipients colloidal silicon dioxide, corn starch, lactose monohydrate, magnesium stearate, microcrystalline cellulose, and povidone (24).

Dissolution and solubility data in FaSSGF, FaSSIF-V2, FeSSGF, and FeSSIF-V2 from location A was previously reported (25). Dissolution of each tablet ($n = 12$) in 500 ml of "from scratch" biorelevant media had been performed. For each individual profile, Eq. 21 was fitted to percent dissolved *versus* time data, using Excel Solver (Microsoft, Redmond, WA; version 2206). Solver is a free Microsoft Excel add-in program from Microsoft and is intrinsic to Excel, although may need to be initially loaded into Excel. In Eq. 21, regression fit k_d, while dose (M_0) was 200 mg, volume (V) was 500 ml, and solubility (c_s) was assigned from solubility measurement. Profiles reached terminal dissolution value at differing times. Hence, fits to profiles employed dissolution data up to and including 30 min (for ibuprofen/FaSSIF-V2, ibuprofen/FeSSIF-V2, ketoconazole/FaSSGF, and ketoconazole/FaSSIF-V2) or 60 min (for ibuprofen/FaSSGF, ibuprofen/FeSSGF, ketoconazole/FeSSGF, and ketoconazole/FeSSIF-V2).

Simulations of the Effect of Dose on Dissolution Profile

In order to complement fits to ibuprofen 200 mg and ketoconazole 200 mg tablet dissolution profiles, simulations in each 900 ml and 250 ml were performed to assess the effect of dose on dissolution profile. Using Eq. 21, simulations varied dose (i.e., 1, 10, 100, and 1000 mg) and drug solubility (i.e., 0.01, 0.1, 1, and 10 mg/ml). Simulations employed a k_d range of 0.01 to 10 ml/mg per min, as fits to observed data below show k_d ranged from 0.0154 to 4.59 ml/mg per min.

Results

Ibuprofen 200 mg and Ketoconazole 200 mg Tablet Dissolution Profiles: Profile Fits

Figures 1, 2, 3, and 4 plot the observed and fitted dissolution profiles into FaSSGF, FaSSIF-V2, FeSSGF, and FeSSIF-V2, respectively. As noted in Table I, ibuprofen/FaSSGF (Fig. 1), ketoconazole/FaSSIF-V2 (Fig. 2), and ketoconazole/FeSSIF-V2 (Fig. 4) showed incomplete dissolution due to inability of 500 ml of media to completely solubilize drug dose of 200 mg. Nevertheless, the Polli dissolution equation (i.e., Eq. 21) was able to adequately fit profiles. The median r^2 (from $n = 12$ profiles) for ibuprofen in FaSSGF, FaSSIF-V2, FeSSGF, and FeSSIF-V2 was 0.98, 0.98, 0.88, and 0.98, respectively, and median r^2 (from $n = 12$ profiles) for ketoconazole in FaSSGF, FaSSIF-V2, FeSSGF, and FeSSIF-V2 was 0.99, 0.69, 0.95, and 0.96, respectively.

In Fig. 2, the fit of ketoconazole in FaSSIF-V2 was dominated by c_s, where c_s anticipated only 1.3% of dose to dissolve, although 2.1% dissolved (Table I), resulting in a relatively low r^2 (median $r^2 = 0.69$); however, observed and fitted profiles were close (Fig. 2). The fit with the largest difference between observed and fitted profiles was ibuprofen/FeSSGF, reflecting the shape of Eq. 21 was less able to accommodate the more linear observed dissolution profile (Fig. 3). Overall, Eq. 21 was able to adequately fit profiles.

Ibuprofen 200 mg and Ketoconazole 200 mg Tablet Dissolution Profiles: Impact of c_s on k_d

Table I lists mean k_d values from fits, where drug/medium are listed in Table I in order of solubility, from highest to

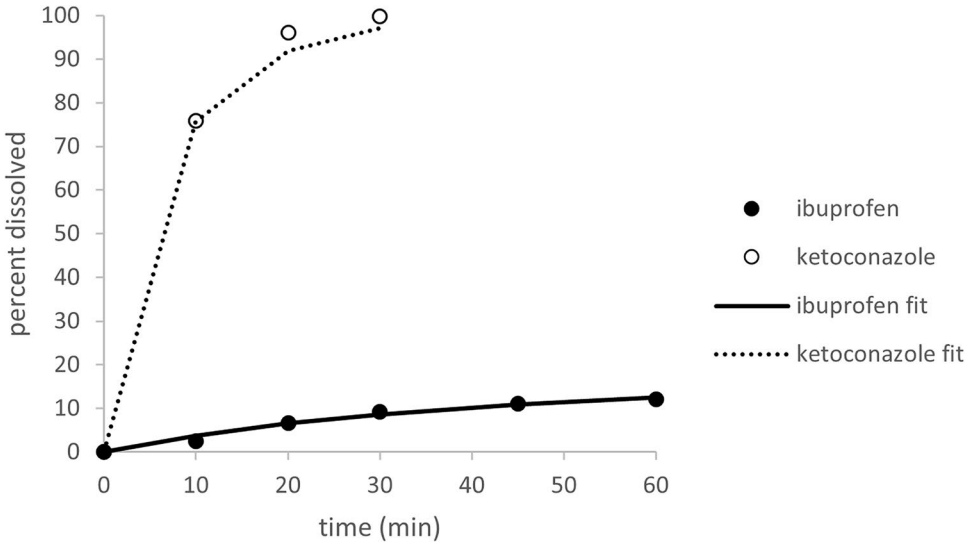

Fig. 1 Observed and fitted dissolution profiles into FaSSGF. Ibuprofen dissolution reflected that only 16.2% of 200 mg dose was soluble in the 500 ml of dissolution media. Fits used Eq. 21, where the maximum percent dissolved was determined solely by drug solubility (Table I)

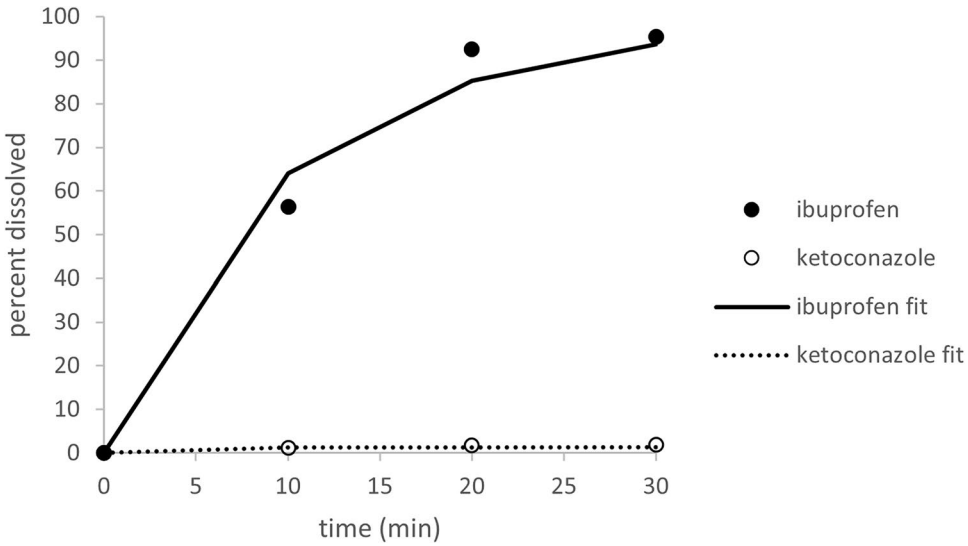

Fig. 2 Observed and fitted dissolution profiles into FaSSIF-V2. Ketoconazole dissolution reflected that only 1.3% of 200 mg dose was soluble in the 500 ml of dissolution media

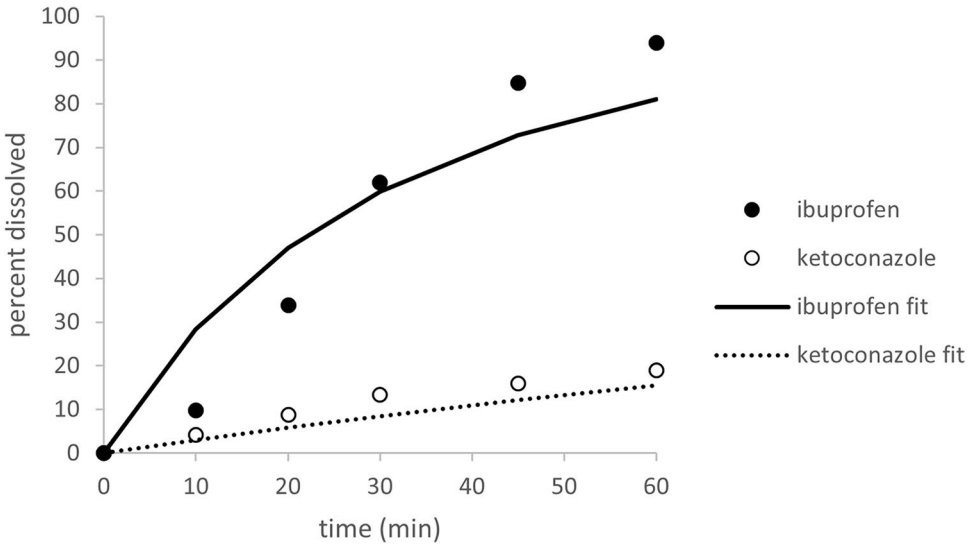

Fig. 3 Observed and fitted dissolution profiles into FeSSGF. Both profiles reflect that FeSSGF colloids are large and slowly diffusing, such that drug dissolution was slow. For each drug, k_d was the slowest in FeSSGF than any other biorelevant media. Dissolution was also slowed, particularly for ketoconazole, since non-sink conditions prevailed (i.e., ibuprofen and ketoconazole required 169 ml and 359 ml FeSSGF to completely dissolve)

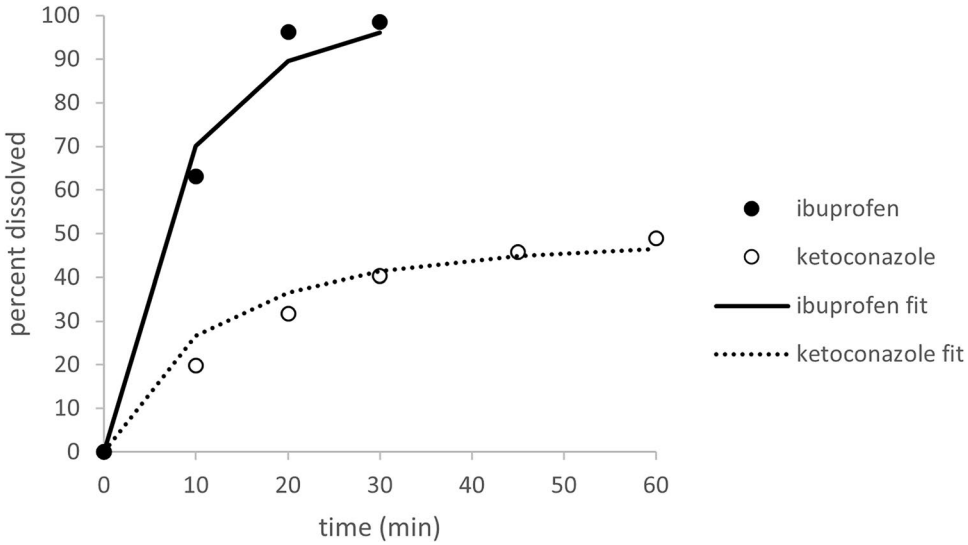

Fig. 4 Observed and fitted dissolution profiles into FeSSIF-V2. Ketoconazole dissolution reflected that only 48.2% of 200 mg dose was soluble in the 500 ml of dissolution media

Table I Mean k_d Values from Fits to Ibuprofen 200 mg and Ketoconazole 200 mg Tablet Dissolution Profiles. Mean and Standard Error of the Mean (SEM). Also Listed Are Drug Solubility, as well as Observed Terminal Percent Dissolved at 60 min and Expected Terminal Percent Dissolved Based on Solubility. Drug/Medium Are Listed in Order of Solubility, from Highest to Lowest

Drug/medium	Solubility (mg/ml)	Observed terminal percent dissolved	Expected terminal percent dissolved based on solubility	k_d (SEM) (ml/mg per min)
Ketoconazole/FaSSGF	11.2	99.0	100	0.0154 (0.0024)
Ibuprofen/FeSSIF-V2	1.76	97.4	100	0.0780 (0.0048)
Ibuprofen/FaSSIF-V2	1.57	94.2	100	0.0732 (0.0034)
Ibuprofen/FeSSGF	1.18	93.8	100 (requires 169 ml FeSSGF to dissolve dose)	0.0303 (0.0023)
Ketoconazole/FeSSGF	0.558	14.0	100 (requires 359 ml FeSSGF to dissolve dose)	0.0550 (0.0007)
Ketoconazole/FeSSIF-V2	0.193	52.9	48.2	0.247 (0.021)
Ibuprofen/FaSSGF	0.0650	12.1	16.2	0.0668 (0.0019)
Ketoconazole/FaSSIF-V2	0.00518	2.1	1.30	4.59 (1.38)

lowest. As perhaps expected, k_d was generally smaller when c_s was larger, as the two parameters are collinear.

Drug solubility ranged over 1000-fold, from 11.2 mg/ml for ketoconazole in FaSSGF to 0.00518 mg/ml for ketoconazole in FaSSIF-V2. Per Eq. 3, dissolution rate is determined by the product of k_d, mass undissolved, and drug solubility, at least initially. Similarly, under sink conditions, the fitted value of k_d will be impacted by the value of c_s. In Table I, the two highest solubility scenarios are ketoconazole/FaSSGF ($c_s = 11.2$ mg/ml) and ibuprofen/FeSSIF-V2 ($c_s = 1.76$ mg/ml). Sink conditions prevailed in each scenario (e.g., only 114 ml FeSSIF-V2 needed to dissolve dose). For this comparison, k_d was smaller when c_s was larger (i.e., ketoconazole/FaSSGF $k_d = 0.0154$ ml/mg per min was smaller than ibuprofen/FeSSIF-V2 $k_d = 0.0780$ ml/mg per min).

This trend was generally observed across Table I. The smallest k_d was for the scenario with the highest solubility, ketoconazole/FaSSGF; the largest k_d was as for the scenario with the lowest solubility, ketoconazole/FaSSIF-V2. Of note, individual estimates for ketoconazole/FaSSIF-V2 k_d varied widely, reflecting rapid achievement of the low terminal extent of dissolution, but were at least 0.420 ml/mg per min for any individual profile.

An exception to this trend were both drugs in FeSSGF, where ibuprofen/FeSSGF yielded a relatively low $k_d = 0.0303$ ml/mg per min and ketoconazole/FeSSGF yielded a relatively low $k_d = 0.0550$ ml/mg per min. Here, drug dissolution rate is assumed to be limited by diffusion of drug-loaded FeSSGF colloid from drug particle to bulk solution. But, FeSSGF colloids are large and slowly diffusing relative to other biorelevant media colloids (26). In the context of results in Table I, a relatively low k_d for dissolution in FeSSGF is consistent with FeSSGF colloid being large and slowly diffusing.

The other exception to the trend was ibuprofen/FaSSGF, where limited solubility anticipates that only 16.2% of dose can dissolve. Fitted k_d was only 0.0668 ml/mg per min. The reason for this exception to the observed trend is unknown.

However, this perhaps slower than expected dissolution k_d for ibuprofen/FaSSGF is a reminder of the simplified dissolution model underpinning this analysis (i.e., Eq. 3). That is, other potential considerations were not explicitly considered (e.g., effect of excipients and tablet manufacturing process). For example, relative to other biorelevant media, FaSSGF has a very low pH of 1.6, which could result in excipients in ibuprofen tablets, or the tablet structure of ibuprofen tablets, to slow drug dissolution, beyond the pH effect on ibuprofen c_s.

Simulations of the Effect of Dose on Dissolution Profile

Table II summarizes results from simulations in 900 ml using Eq. 21 where dose was varied across four levels (i.e., 1, 10, 100, and 1000 mg), c_s was varied across four levels, and k_d was varied across four levels. Given the above potential collinearity of c_s and k_d, dose effect was inspected in Table II across the range of k_d values, for each drug solubility level. As expected, qualitatively, dose effect ranged from essentially no effect at high solubility to pronounced effect at low solubility. For example, in Table II, there was essentially no dose effect when $c_s = 10$ mg/ml, since that high solubility resulted in rapid (i.e., 85% in 30 min) and complete dissolution for even the most dissolution adverse condition of 1000 mg and $k_d = 0.01$ ml/mg per min.

Figures S1-4 in Supplementary Materials plots all 900 ml simulation results. Selected simulations in each 900 ml and 250 ml are discussed immediately below, which employed doses (M_0) of 1, 10, 100, and 1000 mg.

Figure 5 plots the impact of dose on dissolution profile into 900 ml (panel A) and 250 ml (panel B) when drug solubility $c_s = 1$ mg/ml and $k_d = 0.1$ ml/mg per min. For 900 ml simulations, there was essentially no dose effect, other than slightly incomplete dissolution for 1000 mg. One milligram, 10 mg, and 100 mg were rapidly dissolving. From Fig S2, simulation in 900 ml implicates that $k_d = 0.01$ ml/mg per min is probably too low for most IR applications when $c_s = 1$ mg/ml. Compared to 900 ml, the dose most impacted by a lower dissolution profile in 250 ml was 1000 mg (panel B of Fig. 5).

Figure 6 plots the impact of dose on dissolution profile into 900 ml (panel A) and 250 ml (panel B) when drug solubility $c_s = 0.1$ mg/ml and $k_d = 1$ ml/mg per min. Figure 7 uses the same simulation parameters as Fig. 6, except $k_d = 0.1$ ml/mg per min. In each Figs. 6 and 7, there was a dose effect for 900 ml simulations. With progressively slower k_d, each profile progressively slowed (Fig S3). This sensitivity to k_d contrasts with the relative insensitivity of dissolution to k_d when c_s was 10 mg/ml (Fig S1) or 1 mg/ml (Fig S2). Overall, simulations in 900 ml implicate that a k_d value of 0.1 ml/mg per min is low but plausible when $c_s = 0.1$ mg/ml. Compared to 900 ml, the dose most impacted by a lower dissolution profile in 250 ml when $c_s = 0.1$ mg/ml was the 100 mg dose for each $k_d = 1$ ml/mg per min and $k_d = 0.1$ ml/mg per min (panel B of Fig. 6 and panel B of Fig. 7, respectively).

Figure 8 plots the impact of dose on dissolution profile into 900 ml (panel A) and 250 ml (panel B) when drug solubility $c_s = 0.01$ mg/ml and $k_d = 10$ ml/mg per min. For 900 ml simulations, there was a large dose effect, and sink conditions prevailed only for the 1 mg dose. With the low c_s value, dissolution of the 1 mg dose with k_d of 10 ml/mg per min was rapid, but just minimally. Simulations in 900 ml implicate that $k_d = 1$ ml/mg per min is low but plausible value when $c_s = 0.01$ mg/ml (Fig S4). Compared to 900 ml, the dose most impacted by a lower dissolution profile in 250 ml was 10 mg (panel B of Fig. 8).

Agreement Between Observed Dissolution Profiles and Simulations: Implications About k_d

A general trend from observed dissolution profile fits in Table I is that k_d was generally smaller when c_s was larger. k_d ranged from 0.0154 to 4.59 ml/mg per min from the highest to lowest drug solubility scenarios, respectively. Hence, simulations employed a k_d range of 0.01 to 10 ml/mg per min. Four observations about k_d are described in Table I and discussed below relative to fits of observed dissolution profiles.

From $c_s = 10$ mg/ml simulations in 900 ml, it was concluded that the high solubility of 10 mg/ml results in rapid and complete dissolution, even for $k_d = 0.01$ ml/mg per min. Only ketoconazole/FaSSGF had a solubility over 10 mg/ml, where immediate and complete dissolution was characterized by a fitted k_d of 0.0154 ml/mg per min. Hence, observed dissolution profile was supportive of simulations.

From $c_s = 1$ mg/ml simulations in 900 ml, it was concluded that $k_d = 0.01$ ml/mg per min is probably too low for most IR applications when $c_s = 1$ mg/ml. Although c_s exceeded 1 mg/ml for several drug/media scenarios, no fitted k_d was less 0.0154 ml/mg per min, supporting this simulation conclusion.

From $c_s = 0.1$ mg/ml simulations in 900 ml, it was concluded that $k_d = 0.1$ ml/mg per min is low but plausible value when $c_s = 0.1$ mg/ml. Ketoconazole/FeSSIF-V2 and ibuprofen/FaSSGF were scenarios with c_s of about 0.1 mg/ml, and their fitted k_d were 0.247 and 0.0668 ml/mg per min, respectively. There was general support from dissolution data of this conclusion from simulations, although dissolution data suggest that $k_d < 0.1$ ml/mg per min when $c_s = 0.1$ mg/ml is possible. These results remind that, even for IR tablets, several factors can slow dissolution, such as excipients and tablet processing effects.

From $c_s = 0.01$ mg/ml simulations in 900 ml, it was concluded that k_d value of 1 ml/mg per min is a low but plausible value for 0.01 mg/ml solubility. Ketoconazole/FaSSIF-V2 scenario had a c_s of about 0.01 mg/ml. Its fitted

Table II Simulation Results of Impact of Dose for 900 ml. Dose Levels Were 1000 mg, 100 mg, 10 mg, and 1 mg. Impact of Dose Was Assessed for Combinations Across a Range of Drug Solubility c_s and Dissolution Rate Coefficient k_d. Units of k_d Are ml/mg per min. Panel A in Figs. 5, 6, 7, and 8 Show Four Selected Scenarios Involving $c_s = 1$, 0.1, or 0.01 mg/ml for Simulation in 900 ml. As a Point of Reference, Using 250 ml Administered Volume for $c_s = 1$ mg/ml, the Dimensionless Dose Number *Do* Has a Value of 4, 0.4, 0.04, and 0.004 for Doses 1000 mg, 100 mg, 10 mg, and 1 mg, Respectively

c_s (mg/ml)	Impact of dose when $k_d = 10$	Impact of dose when $k_d = 1$	Impact of dose when $k_d = 0.1$	Impact of dose when $k_d = 0.01$	Observations about k_d
10	Essentially no dose effect, as the high solubility of 10 mg/ml resulted in rapid (i.e., > 85% in 30 min) and complete for even the most dissolution rate adverse condition of 1000 mg and $k_d = 0.01$ ml/mg per min				10 mg/ml solubility results in rapid and complete dissolution, even for $k_d = 0.01$ ml/mg per min
1	Essentially no dose effect, except c_s was on track to only allow 90% of 1000 mg dose to dissolve. For $k_d = 0.1$ ml/mg per min, 1 mg, 10 mg, and 100 mg were rapidly dissolving. However, for $k_d = 0.01$ ml/mg per min, 1 mg, 10 mg, and 100 mg were very slowly dissolving (< 70% dissolved in 60 min), even though sink conditions prevailed. Figure 5 (panel A) is $k_d = 0.1$ ml/mg per min				$k_d = 0.01$ ml/mg per min is probably too low for most IR applications when $c_s = 1$ mg/ml
0.1	Significant dose effect. All profiles nearly reached plateau immediately (< 5 min), but only 9% and 90% extent dissolution for 1000 mg and 100 mg	Significant dose effect. 1, 10, and 100 mg slowed significantly, although 1 and 10 mg were rapid. Figure 6 (panel A) is $k_d = 1$ ml/mg per min	Significant dose effect. Even 1 and 10 mg were very slowly dissolving. Figure 7 (panel A) is $k_d = 0.1$ ml/mg per min	Significant dose effect, although profiles becoming increasing similar since dissolution < 10%	k_d value of 0.1 ml/mg per min is low but plausible value for 0.1 mg/ml solubility
0.01	Significant dose effect, particularly for extent of dissolution. Sink conditions prevailed only for the 1 mg dose, which exhibited rapid dissolution. Figure 8 (panel A) is $k_d = 10$ ml/mg per min	Significant dose effect. 1 mg and 10 mg slowed dramatically, with dissolution < 50% in 60 min	Significant dose effect, although all profiles < about 10% at 60 min	Significant dose effect, although all profiles < about 1% 60 min	k_d value of 1 ml/mg per min is low but plausible value for 0.01 mg/ml solubility

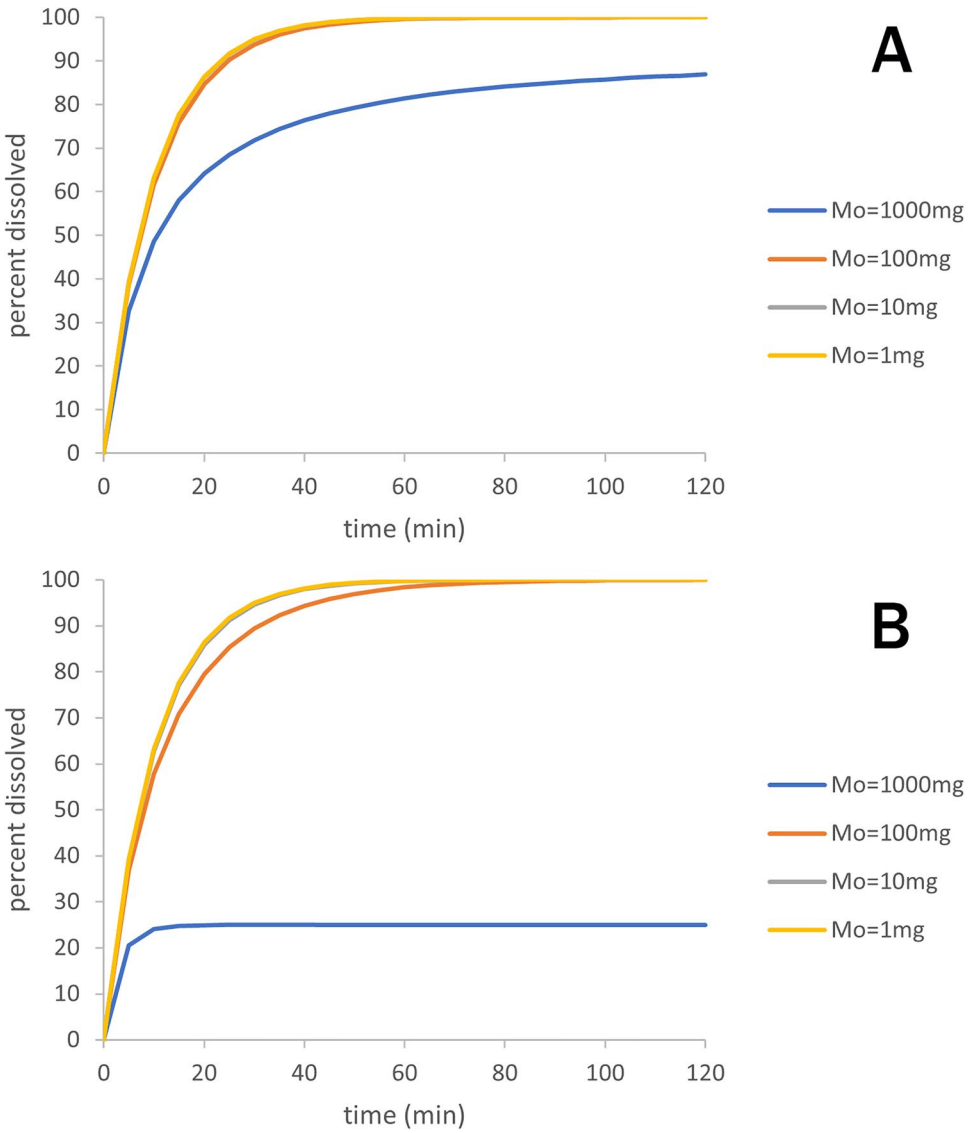

Fig. 5 Impact of dose on dissolution profile into 900 ml and 250 ml when drug solubility $c_s = 1$ mg/ml and $k_d = 0.1$ ml/mg per min. Simulations employed dose (M_0) of 1, 10, 100, and 1000 mg. **A** and **B** are 900 ml and 250 ml, respectively. Compared to 900 ml, the dose most impacted by a lower dissolution profile in 250 ml was 1000 mg

k_d was 4.59 ml/mg per min, in support of the conclusion from simulations.

Overall, there was good agreement between observed dissolution profiles and simulations about the expected range of k_d values of IR products, including k_d trending smaller when c_s is high.

Discussion

Need for Applied Dissolution Equations that Can Accommodate Non-sink Conditions

IR *in vitro* dissolution media generally provide sink conditions, or at least 85% dissolution in 60 min (1). With the greater utilization of biorelevant media, there is a need for *in vitro* dissolution equations that accommodate and consider non-sink conditions, including incomplete dissolution due to insufficient solubility of all drug dose. Biorelevant media often provides a lower drug solubility than pharmaceutical surfactants.

For example, FaSSIF (pH = 6.5) increased carvedilol solubility only about 1.2-fold, compared to buffer, to 55.9 µg/ml (27). Meanwhile, 1% SLS (pH = 6.8) increased carvedilol solubility about 70-fold, compared to buffer, to about 1400 µg/ml (28). FaSSIF increased griseofulvin solubility only about 3%, compared to buffer, to about 12 µg/ml (29). Meanwhile, 1% SLS increased griseofulvin solubility about 85-fold to about 941 µg/ml (30). Posaconazole solubility at pH 6.5 is 0.27 µg/ml (31). FaSSIF and 0.3% SLS increased posaconazole solubility to 1.7 µg/ml and 31.2 µg/ml, respectively (32). Cinnarizine solubility at pH

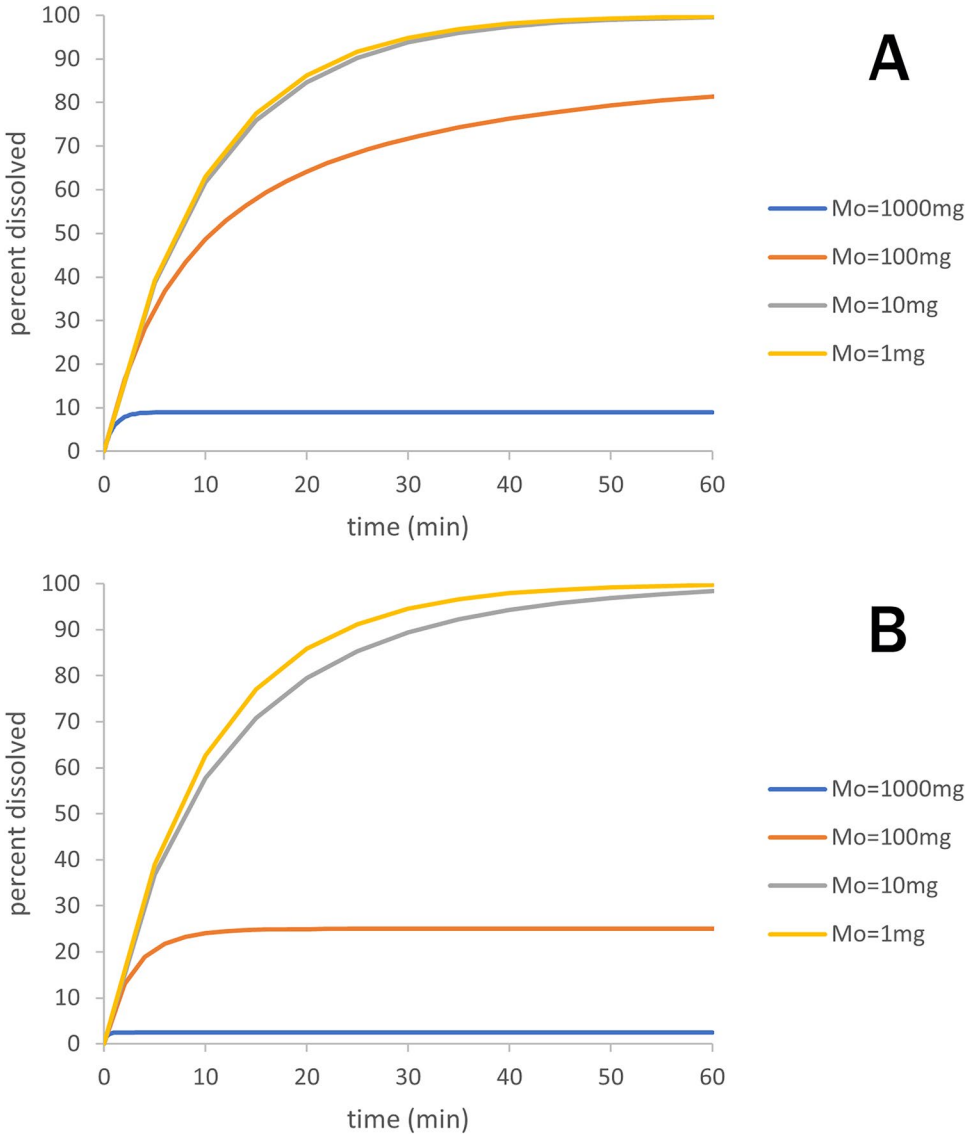

Fig. 6 Impact of dose on dissolution profile into 900 ml and 250 ml when drug solubility $c_s = 0.1$ mg/ml and $k_d = 1$ ml/mg per min. **A** and **B** are 900 ml and 250 ml, respectively. Compared to 900 ml, the dose most impacted by a lower dissolution profile in 250 ml was 100 mg

6.5 is 0.16 µg/ml (33). FaSSIF-V2 and 2% SLS increased cinnarizine solubility to 2.82 µg/ml and 120 µg/ml, respectively (34).

Utility and Advantages of Polli Dissolution Equation

In general, one major application of equation fitting is to summarize data (i.e., data reduction) (35). Dissolution data is frequently subjected to equation fitting, with subsequent analysis such predicting absorption, physiologically based biopharmaceutics modeling (PBBM), *in vitro-in vivo* correlation, or comparison of dissolution profiles (36–40). For example, the FDA guidance on IR dissolution testing recognizes model-depended approaches compare profiles (1). The Hixson-Crowell equation has been used to compare profiles (5). In forecasting the *in vivo* impact of roller compaction scale up, dissolution data was fit to several dissolution equations, including a modified Higuchi equation (41, 42). Carducci has described the development of a real-time-release testing strategy that involves curve fitting to dissolution profiles, followed by regression of the curve fit parameters against the critical material attributes, critical processing parameters, and/or near-infrared (NIR) data (43). In similar cases, the Polli dissolution equation (i.e., Eq. 21, or Eq. 3) has potential application. Figure S5 shows the impact of k_d value on potential "safe space" dissolution profiles into 900 ml when drug solubility $c_s = 0.1$ mg/ml and dose = 10 mg.

Also, a shown here, the Polli dissolution equation has utility in fitting and summarizing dissolution data with a single parameter, when c_s is known and regardless of sink condition prevailing or not prevailing. With only a fit single parameter, potential for model over-parameterization or poor model identifiability is low. Some other dissolution equations, such as Weibull equation, have at least two fitted

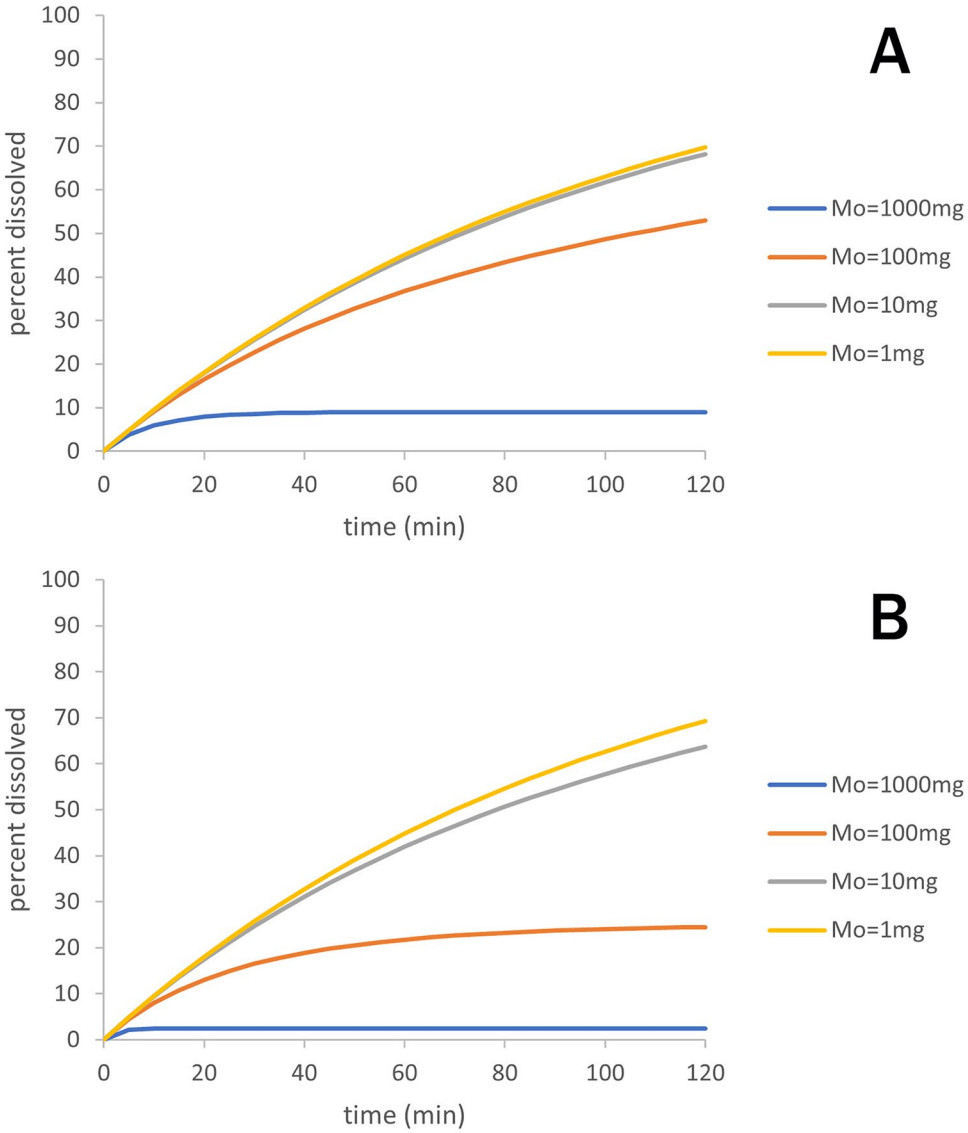

Fig. 7 Impact of dose on dissolution profile into 900 ml and 250 ml when drug solubility $c_s = 0.1$ mg/ml and $k_d = 0.1$ ml/mg per min. **A** and **B** are 900 ml and 250 ml, respectively. Compared to 900 ml, the dose most impacted by a lower dissolution profile in 250 ml was 100 mg

parameters, which can be a disadvantage in data reduction, particularly if such data summarization is intended to be used in subsequent analysis (e.g., profile comparisons, a real-time-release testing strategy, parameter sensitivity assessment). The Polli dissolution equation is a relatively simple, non-differential equation. Excel software was used here to fit dissolution data. Included is an Excel file with instructions for the non-linear regression of the Polli dissolution equation to conventional dissolution data (i.e., percent dissolved *versus* time data). The Excel file requires the free and simple Excel Solver add-in. Since Eq. 21 is the solution to the differential form of the equation (i.e., Eq. 3), software that performs numerical integration is not needed.

Dissolution equations that are applied to percent dissolved *versus* time profiles often do not accommodate sink conditions, since sink conditions are commonplace (4–11). These dissolution equations have also been modified to allow for fitting of an extent of dissolution parameter when dissolution is incomplete (12, 13). Equation 21 intrinsically considers non-sink conditions. No extent of dissolution parameter was needed, although c_s was needed.

Comparison of Polli Equation to the First-Order Dissolution Equation

A common equation for fitting percent dissolved *versus* time profiles is the familiar first-order Eq. (44, 45), whose differential and solution forms are, respectively:

$$dM/dt = -k_{first}M \tag{25}$$

$$\%\ dissolved = 100\%\left(1 - e^{-k_{first}t}\right) \tag{26}$$

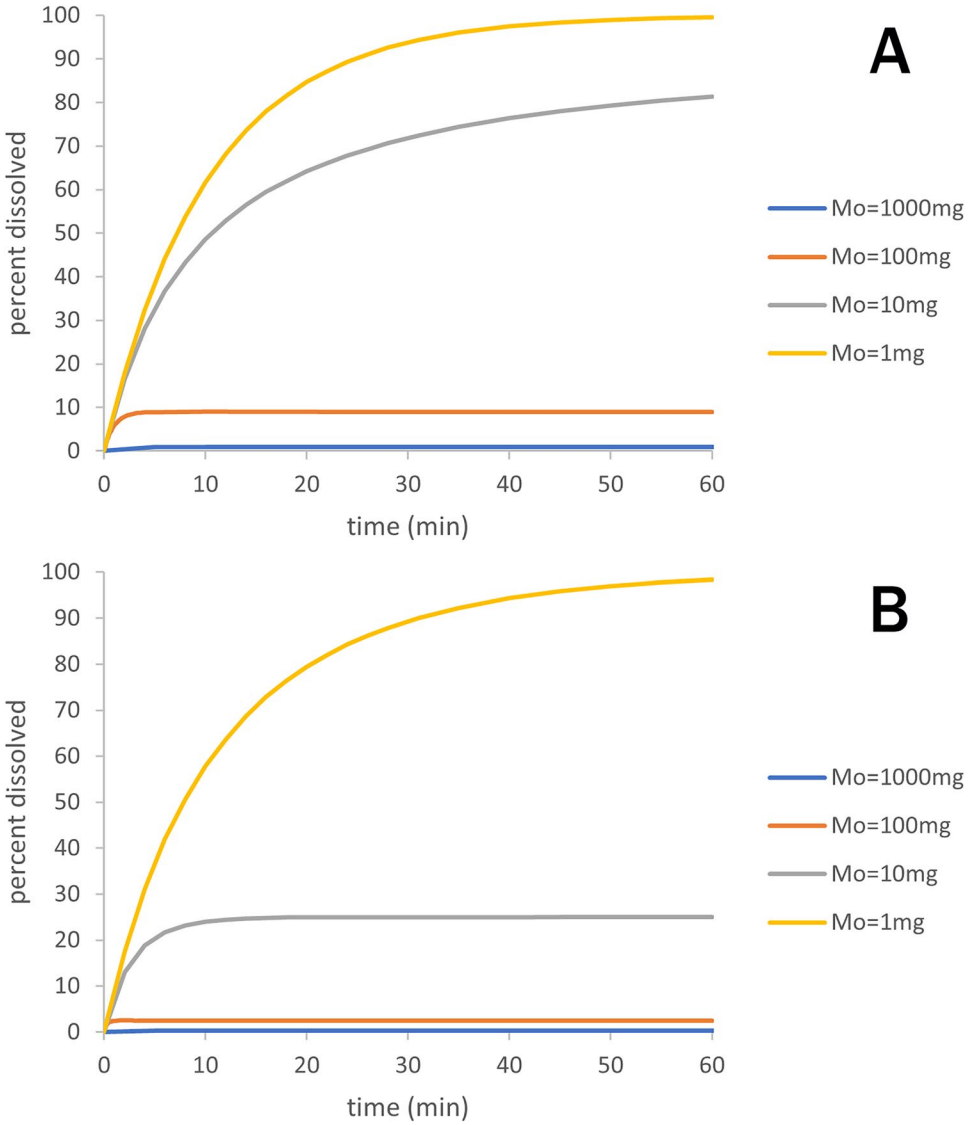

Fig. 8 Impact of dose on dissolution profile into 900 ml and 250 ml when drug solubility $c_s = 0.01$ mg/ml and $k_d = 10$ ml/mg per min. **A** and **B** are 900 ml and 250 ml, respectively. Compared to 900 ml, the dose most impacted by a lower dissolution profile in 250 ml was 10 mg

Equation 3, the differential form of the Polli question, has similarity to the above differential first-order dissolution equation (i.e., Eq. 25). Both are more applied equations than mechanistic equations, although both employ undissolved mass as the driving force for dissolution rate, which is often an acknowledgeable factor of dissolution rate. Under sink conditions, Eq. 3 yields Eq. 22 above, which is practically indistinguishable from the differential first-order equation. However, relative to Eq. 21, a limitation of the first-order equation is that its solution does not accommodate a solubility limit impact on percent dissolved. Of course, such a solubility limit impact can be added to the first-order equation if an impact of solubility on extent of dissolution had been observed or expected, yielding:

$$\%\ dissolved = 100\%\left(\frac{c_s}{M_0/V}\right)\left(1 - e^{-k_{first}t}\right) \tag{27}$$

But, this decision-making is undesirable. Equation 21 has the advantage of not needing to conduct such decision-making, since potential non-sink condition effects are intrinsic to Eq. 21. Equation 21 can be employed in the presence and absence of sink conditions.

Of course, Eq. 21 will not be able to fit many dissolution profile shapes, such as sigmoidal profiles due to slow disintegration. k_d is constant, although could be modified to be a function of time to accommodate other shapes. The Weibull equation is generally recognized as a function that has broad success in fitting a range of dissolution profile shapes. This advantage is in part due to it containing two

fitted parameters (i.e., time factor τ and shape factor β), a potential disadvantage, particularly if such data reduction is intended to be used in subsequent analysis (e.g., dissolution profile comparisons, a real-time-release testing strategy, parameter sensitivity assessment). Additionally, like above for the first-order equation, the Weibull equation does not a *priori* accommodate non-sink condition effects.

Comparison of Polli Equation to the *z*-Factor Dissolution Rate Equation

The z-factor dissolution rate equation with sink conditions is (14, 15):

$$^{dM}/_{dt} = -zM_0^{1/3}M^{2/3}\left(c_s - \frac{M_0 - M}{V}\right) \quad (28)$$

where $z = \frac{3D}{h\rho r_0}$, where z is the particle dissolution z-factor, D is drug diffusion coefficient in the media, h is diffusion layer thickness, ρ is the particle density, and r_0 is the initial particle radius. Although the units of k_d and the particle dissolution z-factor can be considered the same (i.e., ml/mg per min), k_d and z are not identical, by inspection of Eq. 3 *versus* Eq. 28. Equations 3 and 28 differ from one another in that Eq. 3 includes k_dM term, while Eq. 28 includes $zM_0^{1/3}M^{2/3}$ term. In general, in fitting profiles, fitted k_d values can be expected to be greater than fitted z values, since $M < M_0^{1/3}M^{2/3}$ when $t > 0$.

Although Eq. 28 was derived by considering spherical, uniform-sized particle dissolution, it is in practice an applied equation (14,16). For example, Hofsass and Dressman describe z-factor (i.e., z) as a hybrid parameter with potential pitfalls (16), particularly in application to solid oral dosage forms, where particles are typically neither spherical and uniform-sized, nor immediately available for dissolution.

Furthermore, particle size of drug in the formulation is often not available, such that applications of the z-factor dissolution rate equation often do not employ particle size, but rather utilize Eq. 28 for data reduction and simulation (46, 47). For example, Heimbach *et al*. determined the safe space for etoricoxib tablets by employing a PBBM model that used the z-factor dissolution rate equation for data reduction (46). Without regard to particle size, simulations at each pH 6.8 and 2.0 were conducted where z-factor was varied in a in stepwise fashion until the simulated *Cmax* was at least 20% reduced, to define the safe space. Similarly, the z-factor dissolution rate equation was used to fit *in vitro* dissolution data of lesinurad IR tablets, for subsequent pharmacokinetic modeling (47). However, particle distribution was not an input parameter set, but rather a fitted parameter set.

A limitation of Eq. 28 is that the equation is practically only available in the differential form, necessitating the need for software such as GastroPlus, SAAM II, or STELLA that can perform numerical integration (14–17). Compared to z-factor, the Polli equation has the advantage of not needing such software to fit dissolution profiles, as it is an analytical solution and hence does not need numerical integration methods but only regression. Of note, Pepin *et al*. have provided an Excel file with macros to perform numerical integration to fit the z-factor dissolution rate equation, in the context of an approach employing a certain input parameter set (47).

Table III compares characteristics of the Polli equation to the z-factor dissolution rate equation under non-sink conditions, and points towards the simplicity of the Polli equation as a strength. Other particle dissolution rate equations are the Johnson equation and the Wang-Flanagan equation (11,17). Like the z-factor dissolution rate equation, a well-appreciated strength of these equations is ability to simulate particle size effects on dissolution. However, they also require numerical integration to fit dissolution data (14–17). Most particle dissolution models assume spherical shape, which is typically not the case. Drug particle size distribution and shape are often not known in formulated tablets, attenuating the potential advantage of such particle dissolution models, and perhaps creating opportunity for model over-parameterization. Meanwhile, with only a single fitted parameter, Eq. 21 does

Table III Comparison of Characteristics of the Polli Dissolution Equation and the z-Factor Dissolution Rate Equation. Because It Is an Analytical, the Polli Equation Expresses Percent Dissolved as a Function of Time and Can Fit Dissolution Data *via* Non-linear Regression. Meanwhile, the z-Factor Dissolution Rate Equation Is a Differential Equation, Requiring Numerical Integration Methods to Fit the Equation to Dissolution Data

Characteristic	Polli dissolution equation (Eq. 21)	z-factor dissolution rate equation (Eq. 28)
Expression that accommodates sink conditions	$\%\ dissolved = 100\%\left[1 - \frac{(M_0 - c_sV)}{M_0 - c_sVe^{-k_d\left(\frac{M_0 - c_sV}{V}\right)t}}\right]$	$^{dM}/_{dt} = -zM_0^{1/3}M^{2/3}\left(c_s - \frac{M_0 - M}{V}\right)$
Nature of expression	Analytical solution (i.e., not a differential equation, but its integrated solution)	Differential equation
Requirements to fit dissolution data (relative degree of difficulty)	Non-linear regression (simple)	Numerical integration (greater than simple)

not assume any particular particle distribution or shape, but only that drug mass is a driving force for dissolution, with drug solubility (i.e., non-sink conditions) potentially reducing dissolution. Likewise, while z in Eq. 28 can be considered an explicit function of drug diffusion coefficient, which may or may not be known (26, 29), Eq. 21 does not assume any particular drug transport phenomena beyond drug mass as a driving force for dissolution, with potential non-sink effects. Interesting, as noted above, FeSSGF here provided relatively small k_d values, reflecting that FeSSGF colloids are large and slowly diffusing.

Conclusion

The main objective was to derive a dissolution equation for percent dissolved *versus* time that considered non-sink effects, including incomplete solubility in dissolution media. Equation 21 was derived, where the maximum allowable percent dissolved was determined by drug solubility, and without a fitted extent of dissolution parameter. The equation, denoted the Polli dissolution equation, was able to fit ibuprofen and ketoconazole dissolution profiles in biorelevant media, using a single fitted parameter, k_d. Equation 21 was fit to dissolution profiles without regard to sink conditions, and where solubility ranged over a 1000-fold range. k_d was generally smaller when c_s was larger. FeSSGF provided relatively small k_d values, reflecting that FeSSGF colloids are large and slowly diffusing. Simulations showed the impact of non-sink conditions, as well as plausible k_d values for various c_s scenarios, in agreement with observed k_d values. The Polli equation accommodated non-sink condition effects, including whether or not solubility limits dissolution to less than 100%. This accommodate is intrinsic to the equation. The equation has advantages over the use of the first-order and z-factor dissolution rate equations. An Excel file for regression is provided.

Supplementary Information The online version contains supplementary material available at https://doi.org/10.1208/s12248-022-00765-3.

Author Contribution The author conducted the analysis, writing, and approval of the version to be published.

Funding This research was supported by the Food and Drug Administration (FDA) of the US Department of Health and Human Services (HHS) as part of a financial assistance award 5U01FD005946-05 totaling $1,577,013 with 100% funded by FDA/HHS. The contents are those of the author(s) and do not necessarily represent the official views of, nor an endorsement, by FDA/HHS, or the US Government.

Declarations

Conflict of Interest JEP is a member of the Scientific Advisory Board of SimulationsPlus.

References

1. Food and Drug Administration. Dissolution testing of immediate release solid oral dosage forms. 1997. https://www.fda.gov/media/70936/download. Accessed 18 Aug 2022.
2. United States Pharmacopeial Convention Committee of Revision. United States pharmacopeia - national formulary 2022. Rockville, MD: United States Pharmacopeial Convention; 2022.
3. Wu Y, Loper A, Landis E, Hettrick L, Novak L, Lynn K, *et al*. The role of biopharmaceutics in the development of a clinical nanoparticle formulation of MK-0869: a Beagle dog model predicts improved bioavailability and diminished food effect on absorption in human. Int J Pharm. 2004;285:135–46. https://doi.org/10.1016/j.ijpharm.2004.08.001.
4. Siepmann J, Siepmann F. Mathematical modeling of drug dissolution. Int J Pharm. 2013;453:12–24. https://doi.org/10.1016/j.ijpharm.2013.04.044.
5. Polli JE, Rekhi GS, Augsburger LL, Shah VP. Methods to compare dissolution profiles and a rationale for wide dissolution specifications for metoprolol tartrate tablets. J Pharm Sci. 1997;86:690–700. https://doi.org/10.1021/js960473x.
6. Costa P, Sousa Lobo JM. Modeling and comparison of dissolution profiles. Eur J Pharm Sci. 2001;13:123–33. https://doi.org/10.1016/s0928-0987(01)00095-1.
7. Yuksel N, Kanik AE, Baykara T. Comparison of in vitro dissolution profiles by ANOVA-based, model-dependent and -independent methods. Int J Pharm. 2000;209:57–67. https://doi.org/10.1016/s0378-5173(00)00554-8.
8. Lansky P, Weiss M. Does the dose-solubility ratio affect the mean dissolution time of drugs? Pharm Res. 1999;16:1470–6. https://doi.org/10.1023/a:1018923714107.
9. Macheras P, Dokoumetzidis A. On the heterogeneity of drug dissolution and release. Pharm Res. 2000;17:108–12. https://doi.org/10.1023/a:1007596709657.
10. Shekunov B, Montgomery ER. Theoretical analysis of drug dissolution: I. Solubility and intrinsic dissolution rate. J Pharm Sci. 2016;105:2685–2697. https://doi.org/10.1016/j.xphs.2015.12.006.
11. Wang J, Flanagan DR. General solution for diffusion-controlled dissolution of spherical particles. 1. Theory. J Pharm Sci. 1999;88:731–8. https://doi.org/10.1021/js980236p.
12. Usta DY, Incecayir T. Modeling of in vitro dissolution profiles of carvedilol immediate-release tablets in different dissolution media. AAPS PharmSciTech. 2022;23:201. https://doi.org/10.1208/s12249-022-02355-0.
13. Lee H, Park S, Sah H. Surfactant effects upon dissolution patterns of carbamazepine immediate release tablet. Arch Pharm Res. 2005;28:120–6. https://doi.org/10.1007/BF02975147.
14. Nicolaides E, Symillides M, Dressman, Reppas C. Biorelevant dissolution testing to predict the plasma profile of lipophilic drugs

after oral administration. Pharm Res. 2001;18:380–8. https://doi.org/10.1023/a:1011071401306.
15. Takano R, Sugano K, Higashida A, Hayashi Y, Machida M, Aso Y, Yamashita S. Oral absorption of poorly water-soluble drugs: computer simulation of fraction absorbed in humans from a miniscale dissolution test. Pharm Res. 2006;23:1144–56. https://doi.org/10.1007/s11095-006-0162-4.
16. Hofsass MA, Dressman J. Suitability of the z-factor for dissolution simulation of solid oral dosage forms: potential pitfalls and refinements. J Pharm Sci. 2020;109:2735–45. https://doi.org/10.1016/j.xphs.2020.05.019.
17. Johnson KC. Comparison of methods for predicting dissolution and the theoretical implications of particle-size-dependent solubility. J Pharm Sci. 2012;101:681–9. https://doi.org/10.1002/jps.22778.
18. Bou-Chacra N, Melo KJC, Morales IAC, Stippler ES, Kesisoglou F, Yazdanian M, *et al*. Evolution of choice of solubility and dissolution media after two decades of biopharmaceutical classification system. AAPS J. 2017;19:989–1001. https://doi.org/10.1208/s12248-017-0085-5.
19. Rawat S, Jain SK. Solubility enhancement of celecoxib using beta-cyclodextrin inclusion complexes. Eur J Pharm Biopharm. 2004;57(2):263–7. https://doi.org/10.1016/j.ejpb.2003.10.020.
20. Shono Y, Jantratid E, Janssen N, Kesisoglou F, Mao Y, Vertzoni M, *et al*. Prediction of food effects on the absorption of celecoxib based on biorelevant dissolution testing coupled with physiologically based pharmacokinetic modeling. Eur J Pharm Biopharm. 2009;73:107–14. https://doi.org/10.1016/j.ejpb.2009.05.009.
21. Dissolution Methods Database. Food and Drug Administration, White Oak, MD. 2022. https://www.accessdata.fda.gov/scripts/cder/dissolution/index.cfm. Accessed 18 Aug 2022.
22. Mudie DM, Shi Y, Ping H, Gao P, Amidon GL, Amidon GE. Mechanistic analysis of solute transport in an in vitro physiological two-phase dissolution apparatus. Biopharm Drug Dispos. 2012;33:378–402. https://doi.org/10.1002/bdd.1803.
23. Major Pharmaceuticals. Ibuprofen tablets 200mg label. Livonia, MI: Major Pharmaceuticals; 2017.
24. Teva Generics. Ketoconazole tablets 200mg label. Pomona, NY: Teva Generics; 2013.
25. Jamil R, Xu T, Shah HS, Adhikari A, Sardhara R, Nahar K, *et al*. Similarity of dissolution profiles from biorelevant media: assessment of interday repeatability, interanalyst repeatability, and interlaboratory reproducibility using ibuprofen and ketoconazole tablets. Eur J Pharm Sci. 2021;156: 105573. https://doi.org/10.1016/j.ejps.2020.105573.
26. Jamil R, Polli JE. Prediction of in vitro drug dissolution into fed-state biorelevant media: contributions of solubility enhancement and relatively low colloid diffusivity. Eur J Pharm Sci. 2022;173:106179. https://doi.org/10.1016/j.ejps.2022.106179.
27. Fagerberg JH, Tsinman O, Sun N, Tsinman K, Avdeef A, Bergström CA. Dissolution rate and apparent solubility of poorly soluble drugs in biorelevant dissolution media. Mol Pharm. 2010;7:1419–30. https://doi.org/10.1021/mp100049m.
28. Incecayir T. The effects of surfactants on the solubility and dissolution profiles of a poorly water-soluble basic drug, carvedilol. Pharmazie. 2015;70:784–90.
29. Jamil R, Polli JE. Prediction of in vitro drug dissolution into fasted-state biorelevant media: contributions of solubility enhancement and relatively low colloid diffusivity. Eur J Pharm Sci. 2022;174:106210. https://doi.org/10.1016/j.ejps.2022.106210.
30. Sjokvist E, Nystrom C, Alden M, Caram-Lelham N. Physicochemical aspects of drug release. XIV. The effects of some ionic and non-ionic surfactants on properties of a sparingly soluble drug in solid dispersions. Int J Pharm. 1992;79:123–133.
31. Duong TV, Ni Z, Taylor LS. Phase behavior and crystallization kinetics of a poorly water-soluble weakly basic drug as a function of supersaturation and media composition. Mol Pharm. 2022;19:1146–59. https://doi.org/10.1021/acs.molpharmaceut.1c00927.
32. Chen Y, Wang S, Wang S, Liu C, Su C, Hageman M, *et al*. Sodium lauryl sulfate competitively interacts with HPMC-AS and consequently reduces oral bioavailability of posaconazole/HPMC-AS amorphous solid dispersion. Mol Pharm. 2016;13:2787–95. https://doi.org/10.1021/acs.molpharmaceut.6b00391.
33. Berlin M, Przyklenk K, Richtberg A, Baumann W, Dressman JB. Prediction of oral absorption of cinnarizine—a highly supersaturating poorly soluble weak base with borderline permeability. Eur J Pharm Biopharm. 2014;88:795–806. https://doi.org/10.1016/j.ejpb.2014.08.011.
34. Kayaert P, Van den Mooter G. Is the amorphous fraction of a dried nanosuspension caused by milling or by drying? A case study with naproxen and cinnarizine. Eur J Pharm Biopharm. 2012;81:650–6. https://doi.org/10.1016/j.ejpb.2012.04.020.
35. Wagner JG. Pharmacokinetics for the pharmaceutical scientist. 1st ed. Lancaster, PA: Technomic Publishing Company; 1993.
36. Mohamed MF, Winzenborg I, Othman AA, Marroum P. Utility of modeling and simulation approach to support the clinical relevance of dissolution specifications: a case study from upadacitinib development. AAPS J. 2022;24:39. https://doi.org/10.1208/s12248-022-00681-6.
37. Aburub A, Chen Y, Chung J, Gao P, Good D, Hansmann S, *et al*. An IQ Consortium perspective on connecting dissolution methods to in vivo performance: analysis of an industrial database and case studies to propose a workflow. AAPS J. 2022;24:49. https://doi.org/10.1208/s12248-022-00699-w.
38. Mitra A, Parrott N, Miller N, Lloyd R, Tistaert C, Heimbach T, *et al*. Prediction of pH-dependent drug-drug interactions for basic drugs using physiologically based biopharmaceutics modeling: industry case studies. J Pharm Sci. 2020;109:1380–94. https://doi.org/10.1016/j.xphs.2019.11.017.
39. Wu F, Shah H, Li M, Duan P, Zhao P, Suarez S, *et al*. Biopharmaceutics applications of physiologically based pharmacokinetic absorption modeling and simulation in regulatory submissions to the U.S. Food and Drug Administration for new drugs. AAPS J. 2021;23:31. https://doi.org/10.1208/s12248-021-00564-2.
40. Hens B, Seegobin N, Bermejo M, Tsume Y, Clear N, McAllister M, *et al*. Dissolution challenges associated with the surface pH of drug particles: integration into mechanistic oral absorption modeling. AAPS J. 2022;24:17. https://doi.org/10.1208/s12248-021-00663-0.
41. Shesky P, Sackett G, Mahe, L, Lentz KA, Tolle S, and Polli JE. Roll compaction granulation of a controlled-release matrix tablet containing HPMC: effect of process scale-up on robustness of tablets and predicted in vivo performance. Pharm Tech. 1999;23(suppl.): 6–21.
42. Sheskey P, Pacholke K, Sackett G, Maher L, Polli JE. Roll compaction granulation of a controlled-release matrix tablet containing HPMC: effect of process scale-up on robustness of tablets and predicted in vivo performance. Part II Pharm Tech. 2000;24(11):30–52.
43. Zaborenko N, Carducci TM, Ryckaert A, Mandula H, Walworth MJ, *et al*. Predictive dissolution models for real-time release testing: development and implementation – workshop summary report. Dissolution Technolog. 2022;29:150–72. https://doi.org/10.14227/DT290322P150.
44. Polli JE, Crison JR, Amidon GL. Novel approach to the analysis of in vitro-in vivo relationships. J Pharm Sci. 1996;85:753–60. https://doi.org/10.1021/js9503587.
45. Yu XL, Amidon GL. A compartmental absorption and transit model for estimating oral drug absorption. Int J Pharm. 1999;186:119–25. https://doi.org/10.1016/s0378-5173(99)00147-7.
46. Heimbach T, Kesisoglou F, Novakovic J, Tistaert C, Mueller-Zsigmondy M, Kollipara S, *et al*. Establishing the bioequivalence safe space for immediate-release oral dosage forms using physiologically

based biopharmaceutics modeling (PBBM): case studies. J Pharm Sci. 2021;110:3896–906. https://doi.org/10.1016/j.xphs.2021.09.017.
47. Pepin XJ, Flanagan TR, Holt DJ, Eidelman A, Treacy D, Rowlings CE. Justification of drug product dissolution rate and drug substance particle size specifications based on absorption PBPK modeling for lesinurad immediate release tablets. Mol Pharm. 2016;13:3256–69. https://doi.org/10.1021/acs.molpharmaceut.6b00497.